

Ji Y, Hu B, Hill G, Guo W, Blythe PT, Gao L.  
[Signal coordination scheme based on traffic emission.](#)  
*IET Intelligent Transport Systems* 2016, 10(2), 89-96.

**Copyright:**

© 2016 IEEE. Personal use of this material is permitted. Permission from IEEE must be obtained for all other uses, in any current or future media, including reprinting/republishing this material for advertising or promotional purposes, creating new collective works, for resale or redistribution to servers or lists, or reuse of any copyrighted component of this work in other works

**DOI link to article:**

<https://doi.org/10.1049/iet-its.2014.0255>

**Date deposited:**

01/02/2018

# **A study of signal coordination scheme based on traffic emission**

Yanjie Ji<sup>a</sup>, Bo Hu<sup>a</sup>, Graeme Hill<sup>b</sup>, Weihong Guo<sup>b</sup>, Phil Blythe<sup>b</sup>, Liangpeng Gao<sup>a</sup>

a. Jiangsu Key Laboratory of Urban ITS, Southeast University, China

b. Transport Operations Research Group, School of Civil Engineering & Geosciences,  
Newcastle University, UK

## **Abstract:**

This paper presents a new optimal signal coordination scheme with an emphasis on emission reduction as a result of minimized passenger delay. By analyzing the limitation of the algebraic method, a new algorithm using arrival-departure curves was proposed. A microscopic emission simulation platform based on VISSIM (a microscopic multi-modal traffic flow simulation model) and CMEM (Comprehensive Modal Emission Model) was established to estimate traffic emission reduction. A multi-objective genetic algorithm was used to find Pareto solutions that simultaneously reduce both passenger delay and vehicle emissions. Using the real-world traffic data collected in Changzhou city, an example of the signal coordination scheme was developed and its impact on emissions was simulated in the VISSIM-CMEM platform. The simulation results show that the proposed scheme achieved an average emission reduction of 28.8% on public transport vehicles and 18.7% on all vehicles over existing signal schemes.

## **1. Introduction**

Continuous urban development has led to serious traffic congestion and environmental problems associated with traffic emissions. As a major source of air pollution, traffic emissions contribute considerably to the levels of CO, NO<sub>x</sub> and HC in many metropolitan areas [1]. Until recently in China, existing signal algorithms focused on reducing traffic delay with little attention to the impact on traffic emissions.

One technique to reduce congestion is through signal coordination to facilitate the smooth flow of traffic through busy roads. Previous studies have developed methods to realize signal coordination on arterial roads. Qu, et al. [2] proved that a practical and accurate green wave bandwidth could be

set as wide as possible by using a time-space diagram for arterial coordination control. Fan, et al. [3] employed a sensitivity analysis to determine the optimal cycle length for offset optimization. Zhou et al, (2011) used the Webster method to optimize the signal timing and a graphic method to solve the signal phase to reduce the number of stops, traffic delays and to improve the operating speed [4]. He, et al. [5] used PAMSCOD, a unified platoon-based mathematical formulation, to perform arterial traffic signal control in an environment involving buses and automobiles that could communicate with infrastructure.

As the theory and research into signal coordination has developed, some researchers have paid attention to the environment and the emission pollutants caused by traffic [6,7,8] with new methods of real-time measurement and models. Madireddy, et al. [9] demonstrated that reducing speed limits and implementing a signal coordination scheme can achieve emission reduction. De Coensel, et al. [10] suggest that signal coordination schemes can realize a reduction in air pollutants by 10%–40% in the most favourable conditions. In general, these previous studies present different ways to evaluate the impact of signal coordination on emissions, instead of utilizing signal control to reduce the emissions.

CMEM as an effective model to evaluate traffic emissions has been used widely in combination with simulation models. The CMEM model is flexible and can accommodate different types of vehicles and their emission characteristics [11]. Moreover, CMEM has been used to measure the fuel consumption and emissions when combined with micro-simulation software [12]. As acceleration is the main contributor to the increase in particle emissions [13], it seems to suggest that traffic emission must be measured using the combination of CMEM and microscopic simulation software.

Genetic Algorithms (GAs) are an effective method in dealing with multiple objective problems and have been used widely in the study of signal coordination. Girianna and Benekohal [14] applied GAs to solve a dynamic optimization problem formulated by the discrete-time signal-coordination model. Jiao, et al. [15] developed a model framework using GAs to achieve real-time offset and split for the arterial road. Girianna and Benekohal [16] used a micro-genetic algorithm to solve a signal optimization problem associated with the local queues, and generated the optimal signal timing along

the arterial roads required to avoid excessive loading.

As a signal coordination scheme, the passenger delay should not be neglected, so the optimization objectives tend to be emissions and passenger delay. This paper presents a new optimal signal coordination scheme where emission reduction in addition to minimised passenger delay can be considered. Emissions were calculated by spatial interpolation based on the simulated results provided by VISSIM-CMEM platform. A multi-objective genetic algorithm was then conducted by analyzing vehicles' arrival-departure curves in every intersection and calculating corresponding vehicle emissions. This means that the target objectives of emissions and passenger delay can be optimized simultaneously within the algorithm.

## **2. Methodology**

A signal coordination algorithm represented by the algebraic method [17] is configured to maximize green wave bandwidth, however, this does not consider many other factors, such as the discreteness of the traffic flow. Notwithstanding, algorithms based on analysis of arrival-departure curves can take parameters such as delay, number of stops, and operation state of vehicles into consideration which we have shown makes it possible to optimize delay and emission simultaneously.

### **2.1 Analysis of the problems in the maximal green wave bandwidth theory**

With a green wave scheme designed using the maximal green bandwidth theory, it is possible for the green wave bandwidth of real-world traffic to be reduced up to half after progressing through several intersections [17]. This phenomenon suggests that the hypothesis for the maximal green wave bandwidth theory do not take into account the following 4 factors:

- 1) *Random arrival of vehicles*: random fluctuations in the arrival rate of vehicles is crucial to the design of signal offsets, however, it is not reflected in the traditional algebraic methods;
- 2) *Speed variations*: The traditional algebraic methods tend to use the same vehicle speed for both directions of the same road section and have difficulties dealing with terrain or other differences in the surroundings. In reality, the vehicle speed changes according to the road condition, layout and surroundings, as well as the traffic enforcement. The impact of the speed variations needs to be considered for the coordination control of the arterial roads.

- 3) *Discreteness of traffic flow*: In the real world traffic is inherently discrete but traditional algebraic methods work on an abstracted continuous representation. The phenomenon of discreteness will be more apparent with more complex compositions of vehicles and longer distances between intersections. This will exert a greater negative influence on the coordination control proposed by traditional algebraic methods.
- 4) *Residual queue*: when the green time is not long enough to serve all the cars that were waiting at the start of green, the remaining queue at the end of green, namely *residual queue*, grows over a series of cycles and changes dynamically in real-world traffic. This dynamic character cannot be revealed in the algebraic methods.

Due to the lack of flexibility and capability to deal with the above mentioned factors, the algebraic methods are not able to calculate the changes in emissions. Moreover, the algorithm requires that all signal cycles of intersections in arterial roads be the same as the common signal cycle, which leads to the result that intersections with less volume would cause greater delays.

## **2.2 Generation of arrival-departure curves and calculation of evaluation indexes**

### **2.2.1 Departure pattern of the traffic flow in the coordinate system**

The arterial road traffic flow is composed of: through vehicles in the arterial road, left-turn and right-turn vehicles from intersecting roads, this enables the flow to be analysed separately. For through vehicles in the arterial road the departure rate in the road is usually high at beginning of the green light, which corresponds to the dissipation process of queuing vehicles formed during the red light. The flow rate during this period is governed by the capacity of the approaches. When the queue has dissipated, the departure rate in the approach is reduced to the arrival rate, which is typically characterized by a random fluctuation value.

Therefore, the vehicle flow rate along the approaches can be divided into two stages. In the first stage, the flow is uniform with a rate equivalent to the saturation flow rate. In the second stage, the flow is the arrival rate of vehicles. This pattern is the same for the left-turn and right-turn vehicles in intersecting roads. The departure curve on the arterial road is shown in Figure 1 under the hypothesis that the arrival of vehicles on the arterial road and intersecting roads follows a uniform distribution.

By analyzing the departure pattern of the first intersection in the analysis region, the arrival pattern downstream can be determined.

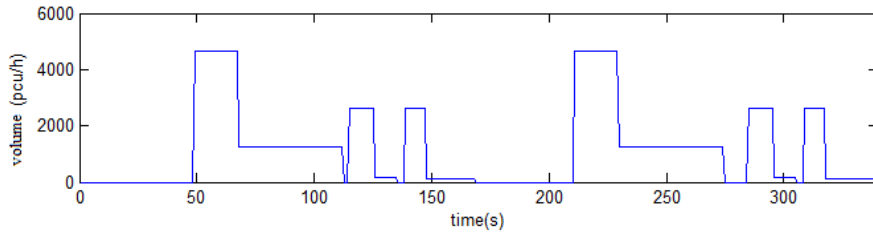


**Figure 1** departure curve of first intersection

### 2.2.2 Arrival pattern of the traffic flow in the coordinate system

After obtaining the departure curve upstream, the arrival pattern in the downstream intersections can be obtained using the method developed by Robertson [18] by considering the discreteness of vehicles on road sections:

$$q_d(j) = \sum_{i=1}^{j-t} q_0(i) F (1-F)^{j-t-i} \quad (1)$$

Where,  $q_d(j)$  is expected arrival rate in the downstream segment d for period j;

$q_0(j)$  is diverging rate in the approach upstream in period i;

t is 0.8 times the average travel time in road section;

F is the dispersion coefficient of the vehicles;

$$F = \frac{1}{1 + A * t} \quad (2)$$

Where, A is a regression parameter, demarcated according to the arrival-departure curve measured from the field.

The arrival curve for the second intersection downstream can be calculated based on the departure curve of first intersection. The arrival curve of the second intersection is shown in Figure 2. The distance between the intersections is 782m, and the average travel speed in the section is 45km/h.

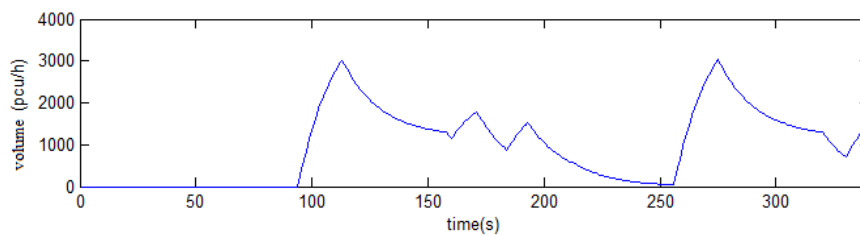


**Figure 2** arrival curve of second intersection

The arrival and departure pattern in the downstream intersections can be calculated in the same way. So we can obtain the arrival and departure curves for each subsequent intersection. The arrival pattern in the first intersection is considered to be random and consequently the arrival pattern for the following approaches, without the influence of the upstream intersections, is thought to be random, too.

### 2.2.3 Calculation of emissions based on analysis of arrival-departure curve

The blue curve in Figure 3 denotes the cumulative number of the arriving vehicles, and the slope of the red curve is determined by the saturation flow rate of the intersection. The area enclosed by these two curves and the time axis is the overall vehicle delay in units of pcu seconds. The pcu value of the intersecting point of the blue and red curves correlates to the number of stops in a signal cycle of the intersection. The delay and number of stops in a signal cycle vary significantly with the change of the offsets in the arterial road. So the influence of offset on vehicles operating can be reflected more comprehensively and quantitatively in the calculation process.

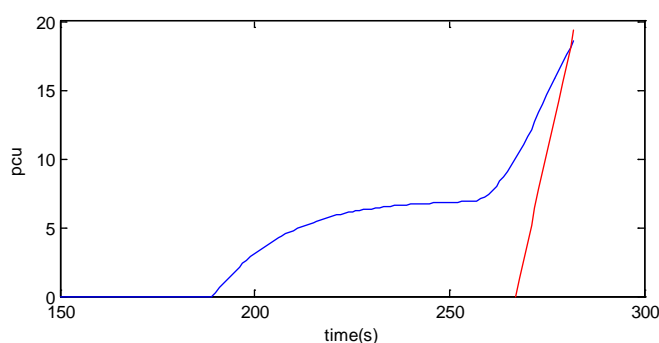


**Figure 3** the curve of cumulative amount of arriving vehicles in intersection B

Previous studies [9, 10] have found that emissions are mainly produced in two stages in the operating process of vehicles. First stage is the starting-up process after the vehicle has stopped. Vehicles will emit more CO, NO and CO<sub>2</sub> in this early period of the driving cycle, and more HC in the middle and later periods. The second important process is when the vehicles accelerate after decelerating where the vehicles is in a high speed. Vehicles will emit more CO, NO and CO<sub>2</sub> in this process. In order to improve computational efficiency and simplify the modelling when using the arrival-departure curve, emissions produced in three processes will be considered: ①vehicles stop and start; ②vehicles

move at a constant speed; ③ vehicles decelerate and accelerate when the speed of the vehicles are higher than average. According to the status of speed and acceleration, emissions can be found through a spatial interpolation method.

There are 4 hypotheses for the arrival-departure curve approach:

- 1) The speed of vehicles in the road section follows a normal distribution. The mean value is the average speed, and the 95th percentile is free flow speed;
- 2) All moving vehicles in road sections between intersections are in state ②, and the acceleration is 0. The speed is allocated randomly according to a normal distribution;
- 3) All vehicles in the area which are surrounded by blue and red curve in Figure 3 experience state ① and their initial speeds are the speeds which operate on road sections. The variation of acceleration is related to the following features of vehicles. In this paper, the acceleration of starting adopts the average acceleration model in VISSIM to simplify the calculation. So the status value of speed and acceleration for every second during the starting process can be obtained.
- 4) In Figure 3, vehicles arriving in the 5 seconds (start-up loss time) after the intersection point of the blue and red curves, which are considered to exhibit a higher than average speed, will experience state ③. It is supposed vehicles will decelerate to the average speed and then accelerate to the initial speed to keep a safe distance when getting close to previously queuing vehicles in the intersection. In this paper, the acceleration adopts the average acceleration model in VISSIM to simplify the calculation, and obtains the status value of speed and acceleration in every second during the starting process.

By simulating the process through Matlab coding, we can obtain the velocity and acceleration of vehicles in different operations. In order to realize the calculation of emissions based on the arrival-departure curve, it is necessary to establish a microscopic emission simulation platform which can obtain the data needed.

### **2.3 Establishment of a microscopic emission simulation platform based on VISSIM and CMEM**

Identifying the mapping relationship of vehicle categories in the VISSIM model and the CEMEM model is the key factor in establishing an effective interface between these two models. For this paper four types of vehicle generated by VISSIM will be studied: car; Light Goods Vehicle (LGV); regular buses; and Bus Rapid Transit (BRT) vehicles. Technical characteristics for corresponding vehicle categories in CEMEM are shown in Table 1. It should be noted that the type 40 (diesel engine light vehicles) in CEMEM is matched with the public transport vehicle. In this paper, a BRT in an arterial road in Changzhou city was used as an analysis example. The BRT vehicles in the case-study city of Changzhou city are large buses, so an extra 7000lbs weight should be added to the type 40 in CEMEM.

The data regarding the running state of vehicles can be output in the form of a database from VISSIM, and then used as the input file to CEMEM after format conversion. Noticeably, the units of the output files in VISSIM are in the metric system, however, the unit of the input files in CEMEM are in the English (Imperial) system. So the metric system should be defined in the model control file of the CEMEM to convert them. The statements to input the file are as follows:

IN\_UNITS=METRIC    OUT\_UNITS=METRIC

**Table 1** The mapping relationship of vehicle categories between VISSIM and CEMEM

Vehicle categories		Vehicle types		Technical characteristics
		defined in	CEMEM model	
Passenger car	Car	5		3-way catalyst, FI(fuel-injected), >50K miles, high power/weight
	LGV	17		Tier 1, light delivery truck, loaded vehicle weight: 3751–5750 lbs
Public transit	Bus	40		Diesel-power, light delivery truck, gross vehicle weight: >8500lbs
	BRT	40		Diesel-power, light delivery truck, gross vehicle weight: >8500lbs

In order to find out the variation tendency of emissions with the change of operating conditions, we

input the data of different velocity and different acceleration into CMEM to simulate emissions under different velocity, acceleration, and type of vehicles.

Emissions can be calculated based on the acceleration-velocity-emissions profile through the spatial interpolation method if the operating states of vehicles are offered. So it becomes possible to calculate the emission and delay simultaneously in the iteration process of signal coordination algorithms.

## 2.4 Calculation of signal coordination scheme based on multi-objective genetic algorithm

The analysis of an example below showed that it's a multi-objective optimization problem to find the solution of a signal coordination scheme whilst considering delay and multiple emissions at the same time. In this problem, the independent variables of the signal scheme that affect the emissions and the travel delay are the common signal cycle and the offset of intersections. So there are N+1 independent variables in the calculation of a signal scheme with N intersections, where each variable is discrete. So a multi-objective genetic algorithm is chosen to calculate the signal scheme in this paper.

### 2.4.1 Multi-objective optimization

There are two or more objective functions in the problem of multi-objective optimization. The problem of multi-objective optimization can be generally described as:

$$\begin{aligned} \min f(x) &= [f_1(x), f_2(x) \cdots, f_i(x)] \\ s.t. x &= \{x \mid g_j(x) \leq 0, j = 1, 2, \dots, m\} \\ x &\in R^n \end{aligned} \quad (3)$$

In general, the result of the multi-objective optimization is a solution set  $\{C, O_1, O_2 \dots O_N\}$ , and no solution which is strictly better than other solutions (not worse in all objectives and strictly better in at least one objective) exist in the set and can be described as: if  $\forall i, f_i(a) \leq f_i(b)$ , and  $\exists i, f_i(a) < f_i(b), i = 1, 2, \dots, t, a \in R^n, b \in R^n$ , then  $a$  is better than  $b$ ; If the solution  $a$  does not exist, then  $b$  is the non-inferior solution or introducing the Pareto solution.  $f(b)$  which is the non-inferior solution of the objective vector space, and all the non-inferior solutions consisting of the Pareto

solution set of the multi-objective optimization problem[19]. In theory, each non-inferior solution could be the optimal solution, and the final result indeed does depend on the specific decision criterion, such as weights of the objectives and of the decision maker. So the basic concept is to find the subset which can approximate to the set of the Pareto solution as closely as possible. Therefore, for our research challenge, the purpose of solving multi-objective optimization problem is to determine the Pareto solution set.

#### 2.4.2 Multi-objective genetic algorithm

A genetic algorithm is utilized here as it is readily modified to deal with multiple objectives by incorporating the concept of Pareto domination in its selection operator, and applying a niching pressure to spread its population out along the Pareto optimal tradeoff surface. The key steps of using multi-objective genetic algorithm to find the solution of signal coordination scheme, or the Pareto solution set of emissions and passenger delay are as follows:

*Chromosome coding.* Denote the independent variables in a signal coordination scheme by a set  $\{C, O_1, O_2, \dots, O_N\}$ , where:  $C$  is the common signal cycle on the arterial road;  $O_i$  is the offset in intersection  $i$ , %. We then construct chromosomes by this methodology to form the population;

*Determine the fitness function.* Use the minimum of total delay and emissions in the inner approaches of coordination control system as the objective function. By transforming the primal problem into a maximization problem to obtain the fitness function. The steps are as follows:

- 1) Searching the maximum delay ( $D_{\max}$ ) or the maximum emissions ( $E_{\max}$ ) in every generation population.
- 2) For an arbitrary individual in a generation population, the value of delay (or emission) is  $D_i$  (or  $E_i$ ). So the fitness function is  $f(D_i) = (D_{\max} - D_i)^l$ .  $l$  varies from 1 to 3 based on actual situation.

When  $l$  equals to 1, it is a typical minimization problem. In order to improve the individual competitiveness, it should be combined with many experiments to determine the value of  $l$ .

### *Selection operation*

#### 1) Individual classification

In this paper, the method NSGAI is used to classify the individuals [20]. For each solution, we calculate two entities dependent on the fitness value: (i)  $e_i$ , the number of solutions which dominate the solution  $i$ , and (ii)  $g_i$ , a set of solutions which the solution  $i$  dominates, where  $i= 1, 2, \dots, p$ ;  $p$  is the number of individuals. We then compare all the individuals and put the individuals which satisfy  $e_i=0$  in level 1. Consequentially we put all individuals in level 1 into the current non-inferiority solution set. For each solution  $i$  in the current non-inferiority solution set, we visit each member ( $j$ ) in its set  $g_i$ . If  $e_j=1$ , then put the individual  $j$  in level 2. We then put all individuals in level 2 into the current. This process continues until all the individuals are classified.

#### 2) Niche calculation

Horn presented the concept of niche which first and foremost is designed to keep the diversity of individuals and prevent local accumulation of the individual solutions [21]. Essentially, because the dimensions vary with the objectives in the multi-objective problem a new method is needed to determine the range of niche. This new method is proposed in this paper. The niche is a rectangular area centred on the location of the individual. For example, consider a problem with  $t$  objectives,  $f_{rl\max}$  and  $f_{rl\min}$  are the maximum and minimum value of the objective function  $r$  in the first generation, so the size of the niche for the objective  $r$  is as follows:

$$d_{r_l} = \frac{f_{rl\max} - f_{rl\min}}{\sqrt[t]{p_0}}, r = 1, 2, \dots, t \quad (4)$$

Where  $p_0$  is the initial population number.

The range of niche in every generation should be determined by calculation.

#### 3) Tournament selection

Choose two individuals randomly. If the level of non-inferiority is different, then choose the relatively high-level (the smaller number of levels) individual. If the levels are the same, then choose the individual in the parse area (with the least number of individuals in niche). In this way, the diversity of the individuals can be kept, and the evolution will develop towards the direction of non-inferior solution and uniform distribution.

#### 4) Crossover operation

This is the main method to generate new individuals in the genetic algorithm. The functions of the crossover operation can generate new individuals by combination and thus reduce the destruction to the effective modes in maximum limit. In our research a two-point crossover operator is used. Generally, a crossover rate between 0.4~0.99 is suggested.

#### 5) Mutation operation

In order to increase the diversity of population and improve the searching ability of the algorithm, inconsistent mutation is used in this paper to improve the global convergent ability in the later period of evolution. The suggested values vary from 0.0001~0.1.

### 3. Case study

In the case study to test the assertion of our research we used the traffic data collected from a BRT route with 8 intersections in the city of Changzhou. This data was used to generate the signal coordination scheme, and from this we evaluated the performance of the scheme by established simulation platforms. The original signal schemes of the intersections obtained from the field survey are shown in the Table 2, which is called scheme #1 for short.

There are 8 intersections in this example, so there are 9 independent variables: 1 variable for common signal cycle length and 8 for offsets of different intersections. According to the traffic volumes of intersections collected in the BRT route, the range of cycle length for each intersection can be obtained based on the signal timing method proposed by Zhang Li, et al.[22], which can reduce traffic delay and the associated emissions during the calculation. Based on the range of a single signal cycle length, the value of common signal cycle range from [132s, 167s], with a step size of one second. The offset of each intersection ranges from [0%, 100%], and the step size is 1%. We set the intersection G as the minor cycle intersection which is derived from the calculation of the results of single intersection signal-timing. Moreover, the signal cycle of intersection G is half of the others in order to realize the signal coordination control. Using these starting points we can find the solution of the signal coordination scheme based upon the multi-objective genetic algorithm, and set the objectives as follows: (i) passenger delay; (ii) The emission of HC; (iii) the emission of NOx; (iv) the emission of CO. The changing trends vary with vehicles' operating condition for the emission of

CO and is similar to the emission of CO<sub>2</sub> and fuel consumption, so the objectives above are enough for study. To test this we first make an optimization for a single objective to discover whether the optimal values of several objectives can be obtained at the same time.

**Table 2** the original signal scheme (scheme #1)

Intersection		A	B	C	D	E	F	G	H
Split (%)		38	38	43	34	54	45	63	66
Original signal scheme (scheme #1)	Offset (%)	42	106	54	19	22	4	108	31
	Cycle length (s)	120	160	130	130	146	146	93	93

### 3.1 Optimization of single objective

The number of individuals in the initial population is 200, and we set the number of evolutionary generation to 200. The mutation operator adopted is the inconsistent mutation. The analysis time for the arrival-departure curve is 1000s.

#### 1) The optimization of passenger delay

To test this we set the fitness function as  $f(D_i) = (D_{\max} - D_i)^2$ , and the function is found to converge after evolving for 97 generations. We now calculate the emission of HC under the solutions which experienced the evolution. The distribution of the possible solutions for the emission of HC and passenger delay is shown in Figure 4(a). It's considered that the optimization of the two objectives can't be obtained at the same time if the value of delay is the minimum, while the emission of HC is not. The justification for this is that when the minimum passenger delay is 70.7s the corresponding emission of HC is 131.7g; whilst with the minimum emission of HC is 121.0g, the passenger delay is 73.6s.

#### 2) The optimization of the emissions

To test this we set the fitness function as  $f(E_i) = (E_{\max} - E_i)^2$ , and found that the function is convergent after evolving for 100 generations. We now calculate the emission of CO under the convergent solution. The distribution of the possible solutions for the emission of CO and HC is shown in Figure 4(b) where the emission of HC is the minimum and the emission of CO is close

to the possible minimum value. To improve the efficiency of operation, the approximate optimization of the two objectives is obtained at the same time. The distribution of the possible solutions for the emission of CO and NO<sub>x</sub> can be considered from the results in the same way, where both the emission of HC and the emission of NO<sub>x</sub> are close to the possible minimum value.

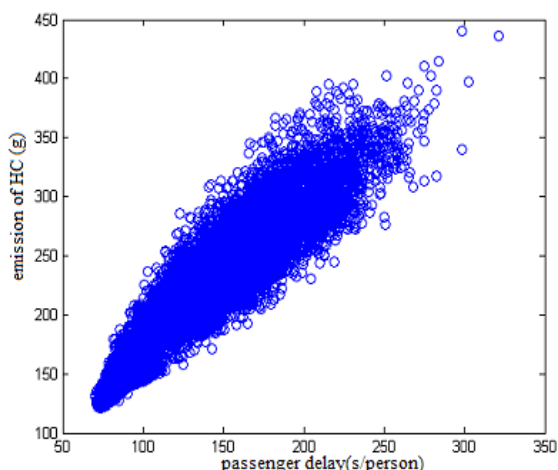


**Figure 4(a)** feasible solution of passenger delay and emission of HC

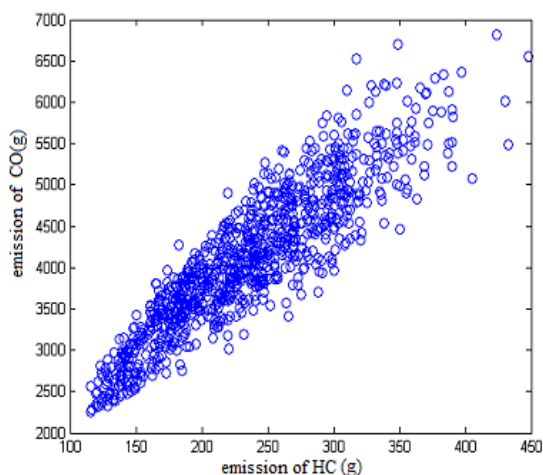


**Figure 4(b)** feasible solution of emission HC and CO

Based on the analysis of the single objective genetic algorithm, the number of objectives was reduced from 4 to 2. The objectives are just the passenger delay and emission of HC, so the efficiency of algorithm can be improved.

### 3. 2 Optimization of multi-objective

As introduced above, a multi-objective genetic algorithm was used based on individual classification and the niche methodology to solve the signal coordination scheme. After initializing the population, the number of individual was set to 200, and the number of evolutionary generations to 200. The function is found to be convergent after evolving for 87 generations. The result of the Pareto solution set for the objectives of passenger delay and emission of HC is shown in Figure 5.

From Figure 5, we find that the passenger delay varies little with the reduction of emission to the left of knee point P, while the passenger delay increases a significant amount with the reduction of emission to the right of point P. So we can conclude that the signal scheme corresponds to the knee point P is thought to be the optimal scheme. The scheme is shown in Table 3.

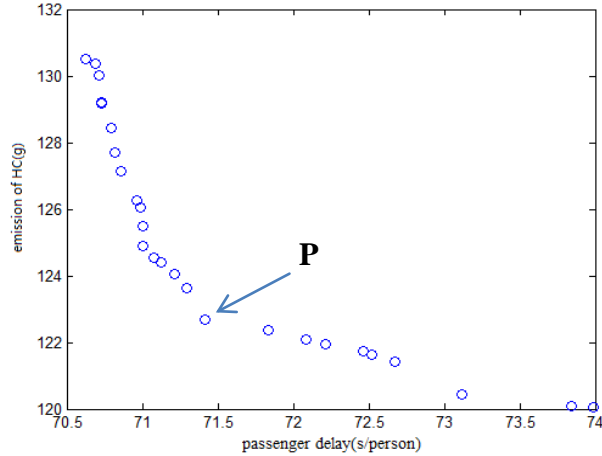


**Figure 5** Pareto solution of multi-objective genetic algorithm

**Table 3** signal coordination scheme based on multi-objective genetic algorithm (scheme#2)

Intersection		A	B	C	D	E	F	G	H
Split (%)		38	38	43	34	54	45	63	66
signal coordination	Offset (%)	105	82	104	47	46	19	58	66
scheme (scheme #2)	Cycle length(s)	157	157	157	157	157	157	79	157

The arrival-departure curves for the partial intersections under the influence of scheme #2 are shown in Figure 6. From Figure 6 we can interpret that the vehicles can basically get through the intersections during the green time, however there are a few vehicles that are forced to stop before the intersections.

In order to make a comparison between the proposed signal coordination and the classical signal coordination scheme, a signal coordination scheme based on classical algebraic method [17] for the case in Changzhou is calculated and shown in Table 4.

To compare this we load the data from the three signal schemes introduced above into the simulation platform VISSIM-CMEM. We obtain the speed and acceleration of vehicles on a second by second basis from VISSIM; moreover we obtain the variation of the weight of the vehicles as passengers boarding and alighting the buses. Finally, we input data from VISSIM to CMEM through the interface established before, and obtain figures for the emissions of each vehicle per kilometer for

each of the different signal schemes.

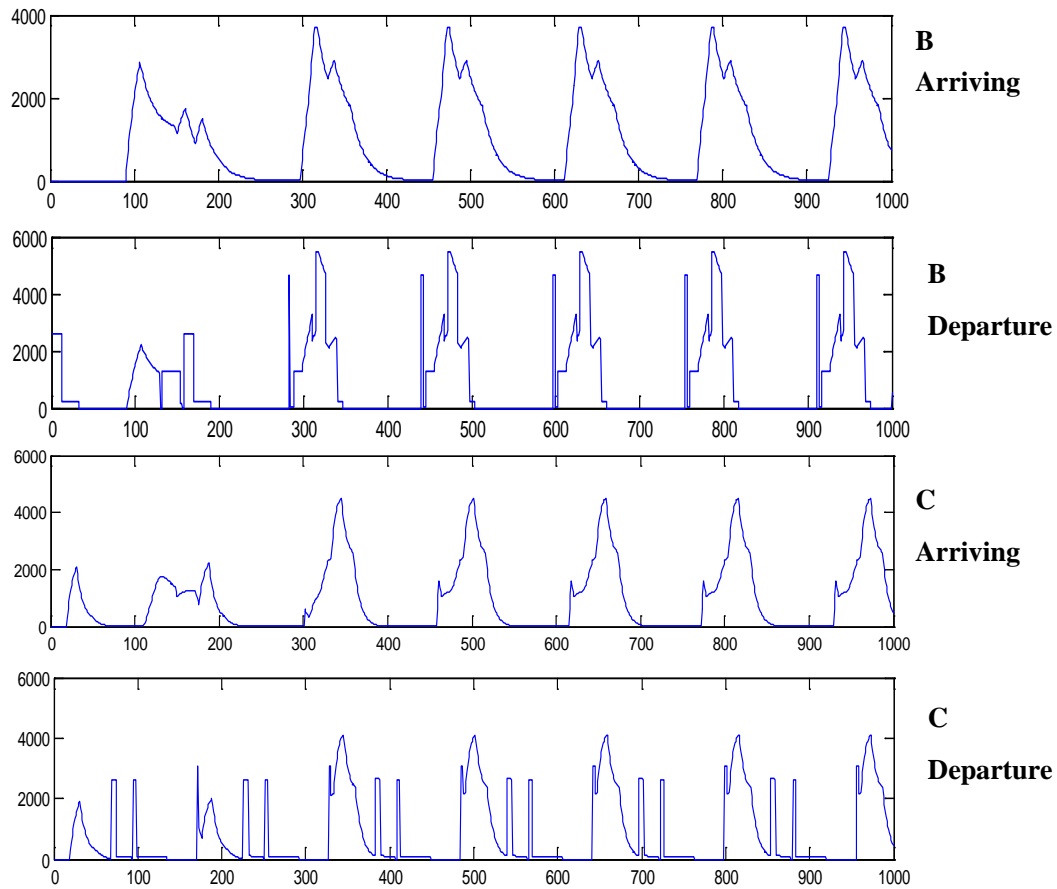


**Figure 6** The arrival-departure curve of intersection B and C from north to south under scheme #2

**Table 4** signal coordination scheme based on classical algebraic method (scheme3)

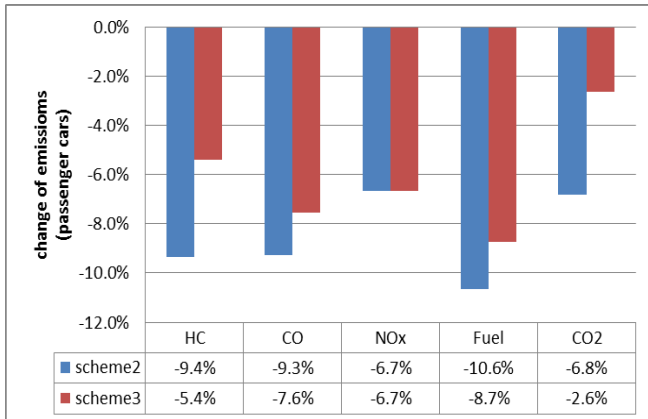
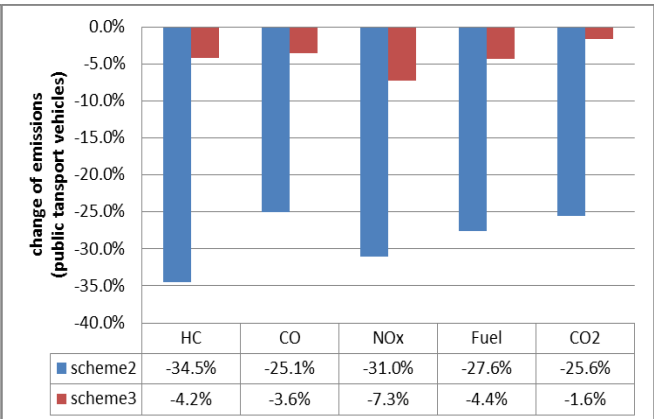
Intersection		A	B	C	D	E	F	G	H
Split (%)		38	38	43	34	54	45	63	66
signal coordination	Offset (%)	39	101	98	40	91	97	23	21
scheme (scheme #3)	Cycle length(s)	125	125	125	125	125	125	125	125

#### 4. Result and discussion

After completing the simulation, the results of emissions, fuel consumption and passenger delay can be obtained, as shown in Table 5. The traffic data examined for the period 4pm to 5pm in Changzhou.

**Table 5** Simulation results of emission, fuel consumption and passenger delay

Scheme	Vehicle categories	HC (g/km)	CO (g/km)	NOx (g/km)	Fuel (g/km)	CO2 (g/km)	Passenger delay(s/p)
Scheme #1	Passenger car	0.962	73.96	0.9	145.6	570	14.30
	Public transit	1.92	4.34	19.54	542.6	2670.12	
Scheme #2	Passenger car	0.872	67.1	0.84	130.1	531.1	14.02
	Public transit	1.257	3.32	13.48	392.6	1987.79	
Scheme #3	Passenger car	0.91	68.37	0.84	132.9	555.01	13.57
	Public transit	1.84	4.27	18.12	518.8	2627.78	

**Figure 7(a)** Change of emission of passenger cars compared to real-world signal plan**Figure 7(b)** Change of emission of public transit compared to real-world signal plan**Figure 7** variation of emission compared to scheme #1

As shown in Table 5 and Figure 7, the scheme (scheme #2) can reduce emissions generated by both public transit and passenger cars compared to a real-world signal scheme (scheme #1), and also has an improvement compared to a signal coordination scheme based on the algebraic method (scheme #3), especially for public transit, which has an improvement of 24.6%. This is because the proposed schemes can reduce the acceleration process which therefore results in less emission. Although the passenger delay in scheme #2 is higher compared to scheme #3, this is due to scheme #3 using a larger signal cycle, specifically a timing method with double the signal cycle time. However the consequential 3.31% increment in passenger delay is deemed not significant, so based upon the results of the research here scheme #2 is considered to be the optimal scheme. Compared to the

real-world signal timing scheme in Changzhou, the proposed scheme could potentially reduce HC emission by 294.2g, CO by 14466.0g, NO<sub>x</sub> by 802.9g, fuel consumption by 6612.3g, CO<sub>2</sub> by 13494.9g based upon the simulation of a one hour time period. Moreover, there is an average reduction of 28.8% on public transport vehicle emissions and an average reduction of 18.7% on all vehicles.

## 5. Conclusion

Following a review of previous work and the assertion that little research has been undertaken to investigate the optimisation of signal coordination to reduce both vehicle emissions and subsequent local pollution levels associated with traffic and vehicle delay. This paper has proposed a method to simulate vehicle emission and delay simultaneously. Based on the simulation method, an algorithm for designing optimal signal coordination scheme is proposed to achieve reductions in both aspects of emission and delay. The main contributions of this paper are listed below:

- 1) Based on the analysis of arrival-departure curves and the characteristics of the exhaust emission, a simple calculation method of the traffic emission based on arrival-departure curves and spatial interpolation method was proposed, in which the emissions can be calculated through the iteration process of changing signal coordination scheme and simulating vehicle operating states.
- 2) In this paper, instead of utilizing the multi-objective weighted sum method, which is widely applied in previous studies, a multi-objective optimization model was built which was designed to find the Parato solutions for the signal coordination scheme.
- 3) Based on the above we propose and test the signal coordination scheme's impact on emission. This is based upon a simulation platform which uses both the VISSIM and the CMEM simulation tools at its heart and with which emissions and fuel consumptions are simulated.
- 4) Results, based upon data provided by the city of Changzhou show that the proposed scheme researched here can reduce the acceleration process of vehicles to improve many aspects of the overall traffic emissions associated with the signal control algorithms, in addition to an improvement in passenger delay. It can realise an average reduction of 28.8% on public transport vehicles emission, an average reduction of 18.7% on all vehicles, and a reduction on passenger delay compared to a real-world signal scheme. There is also an improvement compared to schemes based on the traditional algebraic method and although the passenger delay increased a

little compared to the scheme based on traditional algebraic methods, the corresponding Parato solution acted to reduce both emissions and passenger delay, leaving all the optimal objectives in a favorable state.

Although at an initial stage, this research has clear significance in potentially offering new algorithms that can improve both the transit time through the signalized junction and the associated emission and subsequent traffic pollution. If the results can be further verified and the method optimised then the potential reduction in emissions in Changzhou alone will be significant and translating such a solution to many of the congested (and polluted) cities of China and elsewhere could deliver significant reductions in the harmful pollutants associated with traffic attributed emissions.

### **Acknowledgement**

The financial support from the key project of National Natural Science Foundation of China (No.51338003), the National Key Basic Research Program of China (No. 2012CB725402) and the National Key Technology R&D Program (No.2015BAL02B01) is gratefully acknowledged. The Newcastle University team gratefully acknowledge the financial support from EPSRC from a range of projects that supported this research collaboration: SiDE Digital Hub (EP/G066019/1); TUCP (no. EP/J005649/1); and iBuild (no. EP/K012398/1).

### **Reference**

- 1 Sharma A. R., Kharol S. K., Badarinath K.: 'Influence of Vehicular Traffic on Urban Air Quality—a Case Study of Hyderabad, India', *Transportation Research Part D: Transport and Environment*, 2010, 15 (3), pp. 154-59.
- 2 Qu D.-y., Huang R.-g., Chen X.-f., Li T., Yang X.-r.: 'Algebraic Optimization Method for Arterial Road Signal Coordination Control', in *11th International Conference of Chinese Transportation Professionals (ICCTP)* (2011).
- 3 Fan W., Winkler M., Tian Z. Z.: 'Arterial Signal Timing and Coordination: Sensitivity Analyses, Partition Techniques, and Performance Comparisons', *Advances in Transportation Studies*, 2011, 23.
- 4 Zhou J.: 'Traffic Signal Coordination Control of City Arterial Road That Based on Graphic Method', in *Electronic and Mechanical Engineering and Information Technology (EMEIT), 2011 International Conference on* (IEEE, 2011), pp. 3562-66.
- 5 He Q., Head K. L., Ding J.: 'Pamscod: Platoon-Based Arterial Multi-Modal Signal Control with Online Data', *Transportation Research Part C: Emerging Technologies*, 2012, 20 (1), pp. 164-84.
- 6 Galatioto F., Giuffrè T., Bell M., Tesoriere G., Campisi T.: 'Traffic Microsimulation Model to Predict Variability of Red-Light Running Influenced by Traffic Light Operations in Urban Area', *Procedia-Social and Behavioral*

*Sciences*, 2012, 53, pp. 871-79.

- 7 Galatioto F., Bell M. C., Hill G.: 'Understanding the Characteristics of the Microenvironments in Urban Street Canyons through Analysis of Pollution Measured Using a Novel Pervasive Sensor Array', *Environmental monitoring and assessment*, 2014, 186 (11), pp. 7443-60.
- 8 North R.J. C. J., Wilkins S., Richards M., Hoose N., Polak J.W., Bell M.C., Blythe P., Sharif B., Neasham J., Suresh V., Galatioto F., Hill G.: 'Field Deployment of the Message System for Environmental Monitoring', *Traffic Engineering & Control* 2009, 50 (11), pp. 484-88.
- 9 Madireddy M., De Coensel B., Can A., et al.: 'Assessment of the Impact of Speed Limit Reduction and Traffic Signal Coordination on Vehicle Emissions Using an Integrated Approach', *Transportation Research Part D: Transport and Environment*, 2011, 16 (7), pp. 504-08.
- 10 De Coensel B., Can A., Degraeuwe B., De Vlieger I., Botteldooren D.: 'Effects of Traffic Signal Coordination on Noise and Air Pollutant Emissions', *Environmental Modelling & Software*, 2012, 35, pp. 74-83.
- 11 Xiaoning W., Haiyang L., Tinghui L.: 'The Emission Model of Diesel Bus Based on Cmem in China', *Journal of Harbin Institute of Technology*, 2012, 44 (6), pp. 78-81.
- 12 Mengting W., Tiezhu L.: 'Influence Analysis of Vehicle Fuel Consumption and Exhaust Emission on Bus Lane', *Journal of Transportation Engineering and Information*, 2009, 7 (3), pp. 78-86.
- 13 Sonntag D. B., Gao H. O., Holmén B. A.: 'Comparison of Particle Mass and Number Emissions from a Diesel Transit Bus across Temporal and Spatial Scales', *Transportation Research Part D: Transport and Environment*, 2013, 25, pp. 146-54.
- 14 Girianna M., Benekohal R. F.: 'Using Genetic Algorithms to Design Signal Coordination for Oversaturated Networks', *Journal of Intelligent Transportation Systems*, 2004, 8 (2), pp. 117-29.
- 15 Jiao P., Wang H., Sun T.: 'Real-Time Arterial Coordination Control Based on Dynamic Intersection Turning Fractions Estimation Using Genetic Algorithm', *Mathematical Problems in Engineering*, 2014, 2014.
- 16 Girianna M., Benekohal R. F.: 'Dynamic Signal Coordination for Networks with Oversaturated Intersections', *Transportation Research Record: Journal of the Transportation Research Board*, 2002, 1811 (1), pp. 122-30.
- 17 Roess R. P., Prassas E. S., McShane W. R.: *Traffic Engineering* (Prentice Hall, 2004).
- 18 Robertson D.: 'Traffic Models and Optimum Strategies of Control: A Review', (Transport and Road Research Laboratory, 1979).
- 19 Lianwen Z., Renwei X.: 'The Sufficient and Necessary Conditions of the Pareto Solution', *JOURNAL OF BEIJING UNIVERSITY OF AERONAUTICS AND ASTRONAUTICS*, 1997, 23 (2), pp. 200-05.
- 20 Pires D. F., Antunes C. H., Martins A. G.: 'Nsga-Ii with Local Search for a Multi-Objective Reactive Power Compensation Problem', *International Journal of Electrical Power & Energy Systems*, 2012, 43 (1), pp. 313-24.
- 21 Horn J., Nafpliotis N., Goldberg D. E.: 'A Niche Pareto Genetic Algorithm for Multiobjective Optimization', in *Evolutionary Computation, 1994. IEEE World Congress on Computational Intelligence., Proceedings of the First IEEE Conference on* (Ieee, 1994), pp. 82-87.
- 22 Zhang L., Yin Y., Chen S.: 'Robust Signal Timing Optimization with Environmental Concerns', *Transportation Research Part C: Emerging Technologies*, 2013, 29, pp. 55-71.